Available online at www.sciencedirect.com
ScienceDirect
Journal of Power Sources 160 (2006) 1471–1479
JOURNAL OF POWER SOURCES
www.elsevier.com/locate/jpowsour

Conditions to prepare PPy/Al_2O_3/Al used as a solid-state capacitor from aqueous malic solutions

J.I. Martins [a,*], S.C. Costa [a], M. Bazzaoui [a], G. Gonçalves [b], E. Fortunato [b], R. Martins [b]

[a] *Faculdade de Engenharia, Departamento de Engenharia Química, Universidade do Porto, Rua Roberto Frias, 4200-465 Porto, Portugal*
[b] *Faculdade de Ciências e Tecnologia, Departamento de Ciências e Materiais, CEMOP, Universidade Nova de Lisboa, Caparica, Portugal*

Received 2 February 2006; received in revised form 4 March 2006; accepted 9 March 2006
Available online 6 May 2006

Abstract

The electrosynthesis of polypyrrole (PPy) has been achieved on aluminium in aqueous medium of malic acid by means of cyclic voltammetry, potentiostatic and galvanostatic techniques. Scanning electron microscopy (SEM) and X-ray microanalysis by dispersion energy spectroscopy (EDS) applying on surfaces show that the PPy coating is developed from the metal surface through the cracks of the initial Al_2O_3 layer. Moreover, the results reveal that the homogeneity of the film achieved increases with the time of electropolymerization.

A mechanism involving the participation of the supporting electrolyte and the pyrrole (Py) in distinct active sites was proposed based on the linear sweep voltammetry. It is observed for all the applied electrochemical techniques that the pyrrole concentration has to be higher than 0.1 M to allow the polypyrrole electrodeposition in acid medium.

Scanning electron microscopy, secondary electrons (SE) and backscattering electrons (BE), shows that the PPy coating obtained in galvanostatic and potentiostatic modes starts with small islands at weak applied potentials or current densities. The corrosion results in 3% NaCl medium show that the PPy coating decreases the corrosion behaviour of the aluminium. The bilayer Al_2O_3/PPy shows a capacitor with future applications.

Keywords: Polypyrrole; Aluminium; Malic acid; Corrosion; Capacitor

1. Introduction

Conventional aluminium electrolytic capacitors present some disadvantages such as high impedance and thermal instability, in addition to problems with the liquid electrolyte leakages. To coop this situation, the researchers have improved the development of solid electrolytic capacitors based on MnO_2 [1,2], or complex salts of organic semiconductor and conducting polymers (CP) [3–9]. Polypyrrole is one of the most used CP as counter electrode on aluminium [2,6,9–11] and tantalum [5,12–16] capacitors considering their good adhesion to dielectric films, higher conductivity and excellent stability.

The oxidation of pyrrole has been carried out by either (1) electropolymerization at a conductive substrate by the application of an external current or potential, or (2) chemical polymerization in solution by the use of a chemical oxidant. Photochemical and enzyme-catalyzed polymerization routes have been described but not yet enough developed. From among of all these processes the electropolymerization is only the technique that allows attaining an adherent coating on metallic surfaces. This property is essential when they are used as solid electrolyte in capacitors or as protective coatings on active metals such as iron, copper, zinc, aluminium and their alloys [17–20].

The aluminium supports a thin, compact, passive film of hydroxide and oxides that renders difficult the electropolymerization process of Py on its surface. Some important results were meanwhile obtained by several researches in organic and aqueous media [20–27]. Hülser and Beck [28] have reported that the aluminium has to be pretreated by either a mechanical or an anodic activation before the electropolymerization.

The PPy electrosynthesized on aluminium in aqueous medium is a bilayer-film composed by a barrier-type Al_2O_3 and an electronically conducting PPy film [23]. The formation of Al_2O_3 proceeds at two interfaces, namely at the Al/Al_2O_3 and at the Al_2O_3/PPy. The mechanism of this system is the following: (1) the Al^{3+} is generated at Al/Al_2O_3 interface; (2) the

* Corresponding author.
E-mail address: jipm@fe.up.pt (J.I. Martins).

0378-7753/$ – see front matter © 2006 Elsevier B.V. All rights reserved.
doi:10.1016/j.jpowsour.2006.03.020

obtained cations migrate through growing Al_2O_3 layer toward the solution, while oxide ions (O^{2-}) migrate toward the aluminium electrode [29]. The initial Al_2O_3 layer contains cracks on which its hydrophilic wall is likely attached to the hydrophilic groups of supporting electrolyte. This compound forms a micelle at the surface of the wall of the cracks producing a hydrophobic domain with a highly concentration of pyrrole. It is in these cracks that preferentially pyrrole is electropolymerized to form electronically conducting paths of PPy, which is extended from the Al electrode to the surface of the Al_2O_3 layer.

In this work we investigate the electrodeposition of polypyrrole on oxidizable aluminium in aqueous medium with malic acid [30,31] as supporting electrolyte using several electrochemical techniques. The coated electrodes have been tested to corrosion in sodium chloride medium and as solid electrolytic capacitor

2. Experimental

Pyrrole monomer (Aldrich) was distilled under nitrogen, malic acid, HCl, NaOH and NaCl (>99%) were purchased from Merck and used as received, and water was distilled twice before use.

The electrochemical experiments were performed in a one-compartment cell with three electrodes connected to Autolab model PGSTAT20 potentiostat/galvanostat with pilot integration controlled by GPES 4.4 software. The working electrode rod (1 cm diameter) or sheet (area 2 cm × 2 cm, thickness 0.4 cm) was aluminium 99%. The electrodes were wet mechanically polished successively with 200, 600 and 1000 or 4000 abrasive paper, and rinsed in water before each electrochemical experiment. Following this pretreatment the electrode was immediately transferred to the electrochemical cell. A stainless-steel plate was used as auxiliary electrode. All the potentials were measured versus an Ag/AgCl (0.1 M KCl) reference electrode.

Scanning electron microscopy micrographs were obtained on a JEOL JSM-6301F instrument. The microscope chamber was maintained at a pressure between 4 and 10 Pa. The distance between the sample and the objective lens was remained at 15 mm (working distance). The SEM filament was operated at variable current and a voltage of 15 kV using magnifications 300× and 3000×. The X-ray microanalysis was obtained with the Noran–Voyager equipment.

Electrochemical corrosion measurements were performed at room temperature in 3% NaCl solution. The galvanostatic aluminium dissolution of the naked and PPy-coated electrodes (AA analysis of the cationic species in the solution) was performed in the range of 4–10 mA cm^{-2} applied current densities.

The equivalent parallel resistance (R) and capacity (C_s), together with the leakage current (L_c) of the solid capacitor were measured with a RCL meter (FLUKE PM 6306) and leakage current tester by applying 1 V using a DC power supply (FREAK NP-9615) and a multimeter (KEITHLEY 2000), respectively. The electric contact area (0.07 cm^2) on the PPy layer has been made by thermal evaporation of aluminium. Before the capacity measurements the samples were annealed at 50 °C during 1 h under vacuum.

3. Results and discussion

3.1. Py electropolymerization

3.1.1. Cyclic voltammetry

A previous study on the mechanical pretreatment of the electrodes surfaces in acid medium shows that only with the 4000 emery paper finishing was possible to obtain uniform PPy films. So, in all the trials this mechanical procedure has been used.

The voltammograms of aluminium electrodes submitted to successive potential scans between −1 and 2 V versus Ag/AgCl in {0.2 M $C_4H_6O_5$ + 0.5 M Py} medium with different pH at 100 mV s^{-1} are presented in Fig. 1. At pH 2 the current density

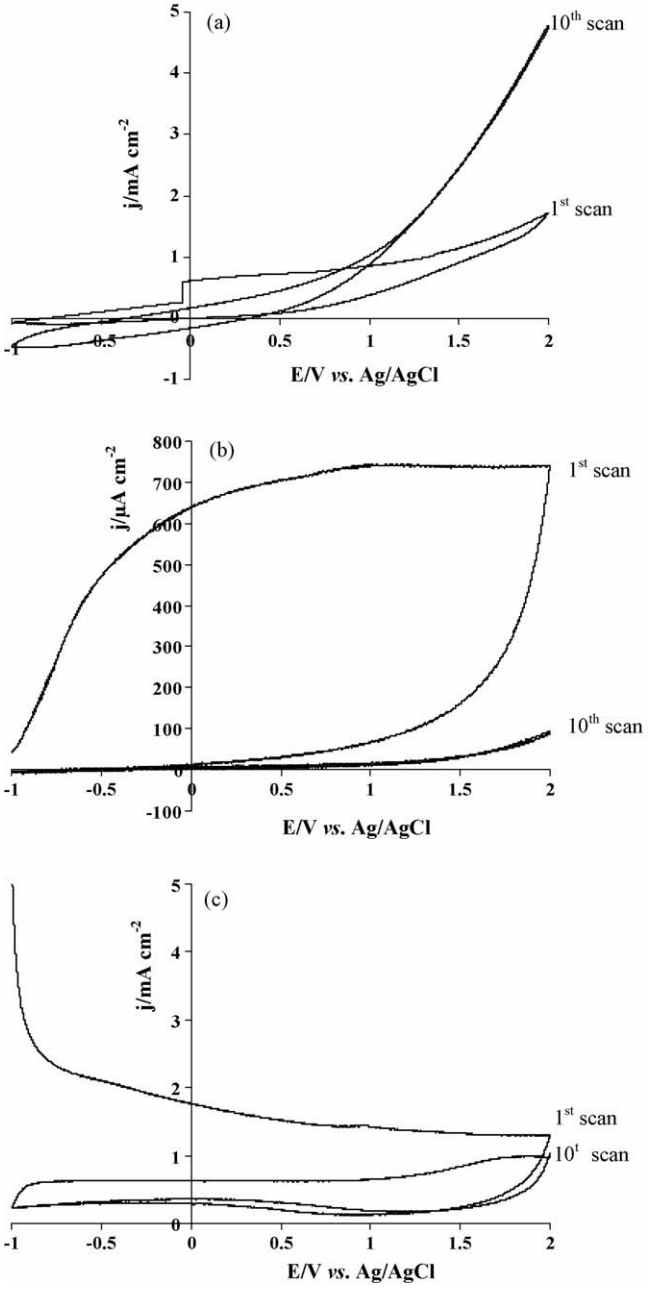

Fig. 1. Cyclic voltammograms of PPy growth on Al in {0.2 M $C_4H_6O_5$ + 0.5 M Py} medium: (a) pH 2; (b) pH 7 and (c) pH 12. Scan rate, 100 mV s^{-1}.

Table 1
Study of the electropolymerization of pyrrole on aluminium electrodes in aqueous malic medium using the voltamperometric technique

Malic acid (M)	Pyrrole (M)	Scan rate (mV s^{-1})	j (mA cm^{-2}) of first scan at $E = 2$ V vs. Ag/AgCl	PPy characteristics after the 10th scan
0.1	0.5	100	0.8	Thin coating
0.2	0.5	100	1.7	Good coating
0.4	0.5	100	3.1	Good coating
0.8	0.5	100	5.5	Good coating
0.2	0.1	100	0.7	No coating
0.2	0.3	100	0.9	Thin coating
0.2	0.8	100	2.5	Good coating

of the oxidation wave increases with each scan indicating the build-up of a conducting electroactive polymer. No film on Al occurred at pH 7 and 12, which can be explained by the behaviour of the support electrode: in neutral pH solution is developed an insoluble and thick film that limits the reactivity of the Al electrode, while at pH 12 the solubility of the aluminium oxide increases as a result of the formation of aluminates [32]. At pH 2 there is also instability of the aluminium oxide but not enough to inhibit the Py electropolymerization.

Potentiodynamic polarization curves were performed to determine the mechanism and kinetics of the anodic polymerization of pyrrole on aluminium electrodes, which mainly details are summarized in Table 1. The current density of the oxidation wave is proportional to the monomer concentration, C_{Py}, which follow the equation:

$$\left(\frac{\partial \log j_p}{\partial C_{Py}}\right)_{E=2\,V} \approx 1 \tag{1}$$

and it is also proportional to the concentration of the supporting electrolyte according with the equation:

$$\left(\frac{\partial \log j_p}{\partial C_{SE}}\right)_{E=2\,V} \approx 1 \tag{2}$$

Based on the experimental results and in the mechanism proposed in the literature [33–35] the following steps are suggested to explain the initial electropolymerization of pyrrole:

$$Mal^- + Z \leftrightarrow Mal^- Z_{ads} \tag{3}$$

$$Py + Z' \leftrightarrow PyZ'_{ads} \tag{4}$$

$$Mal^- Z_{ads} + PyZ'_{ads} \rightarrow Mal^- Py_{ads}{}^{\bullet} + e \tag{5}$$

$$Mal^- Py_{ads}{}^{\bullet} + Mal^- Py_{ads}{}^{\bullet} \rightarrow PPy + 2Mal^- + 2H^+ \tag{6}$$

$$PPy + Mal^- \rightarrow Mal^- PPy^{\bullet} + e \tag{7}$$

$$Mal^- PPy^{\bullet} + Mal^- Py^{\bullet} \rightarrow PPPy + 2Mal^- + 2H^+ \tag{8}$$

According to the mechanism proposed by Naio et al. [23] it is possible to say that malate ion (Mal^-) and Py are adsorbed in distinct active sites Z and Z', respectively, in the Al_2O_3 and Al surfaces. Taking into account the malate structure we admit that its interaction with the substrate happen in only one active site. Now, the theoretical treatment of the kinetic processes of pyrrole electropolymerization can be performed making the following assumptions: (1) the rate-limiting step is Eq. (5); (2) the adsorption of Py and Mal^- on their active sites remains in equilibrium during the electrode reaction. The reaction rate should be then given by the following expression:

$$R = k\theta_1\theta_2 \tag{9}$$

$$j \propto R \tag{10}$$

Using the Langmuir adsorption equation to express the fraction of the area occupied by the pyrrole and malate ions [36]:

$$\theta_1 = \frac{K_1[Mal^-]}{1 + K_1[Mal^-]} \tag{11}$$

$$\theta_2 = \frac{K_2[Py]}{1 + K_2[Py]} \tag{12}$$

Put Eqs. (11) and (12) in Eq. (9), the Eq. (10) can be expressed as:

$$j = k_3 \left(\frac{K_1[Mal^-]}{1 + K_1[Mal^-]}\right)\left(\frac{K_2[Py]}{1 + K_2[Py]}\right) \tag{13}$$

or

$$j = k\frac{[Py][Mal^-]}{1 + K_1[Mal^-] + K_2[Py] + K_1K_2[Py][Mal^-]} \tag{14}$$

with $k = k_3K_1K_2$.

Thus, the current or reaction rate will be proportional to the concentrations of the supporting electrolyte and the pyrrole monomer. Considering that equilibrium adsorption constants of malate ions and pyrrole, respectively, K_1 and K_2, are not much larges, which turns possible to neglect their terms in the denominator of Eq. (14), this equation becomes

$$j = k[Py][Mal^-] \tag{15}$$

with $k = 15.3$ mA cm^{-2} M^{-2} obtained from experimental parameter fitting.

The Eq. (15) is in full agreement with the experimental potentiodynamic results. So, it is reasonable to say that the current or reaction rate is first order with respect to both reactants: the malate ion and the pyrrole.

The Fig. 2 shows that the current density of the oxidation wave of pyrrole decreases with the scan rate. Taking into account to same conditions the voltammograms on Al in solutions without pyrrole, Fig. 3, the plateau established after the aluminium oxidation, about −0.7 V versus Ag/AgCl, is associated with the Al_2O_3 formation. From the observed values of current density at the plateau, we can say for potentials higher than the monomer

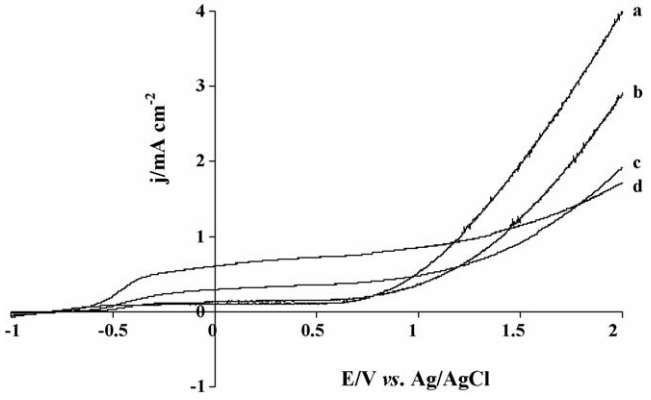

Fig. 2. Linear sweep voltammograms on Al electrode in {0.2 M $C_4H_6O_5$ + 0.5 M Py} medium at pH 2 with different scan rate: (a) 10 mV s^{-1}; (b) 20 mV s^{-1}; (c) 50 mV s^{-1}; (d) 100 mV s^{-1}.

oxidation that the current density is mainly associated with the pyrrole electropolymerization. According to the proposed mechanism, this behaviour may be explained by an increase of the active sites of pyrrole inside the cracks of aluminium oxide, where is developed the nucleation and growing of polypyrrole, with the decrease of the scan rate. The adherence tests performed on the produced PPy films comes to confirm the theoretical analysis, since its values increase significantly with the decay in the scan rate. Indeed, we know from the coatings behaviour that increasing the attached points on the metal surface increases the adherence.

3.1.2. Galvanostatic deposition

PPy can also be formed at a constant current density equal or higher than 1 mA cm^{-2} in {0.2 M $C_4H_6O_5$ + 0.5 M Py} medium at pH 2. Fig. 4 shows that potential linearly increases up to attain a maximum value indicating the formation of a barrier-type Al_2O_3 layer on Al. The time to establish this layer reduces with the applied current density. After then occurs a breakdown of the dielectric and the potential exponentially decays to a plateau pointing out the development of a conducting coating. In the case of the applied current density of 4 mA cm^{-2} it seems to be yet a

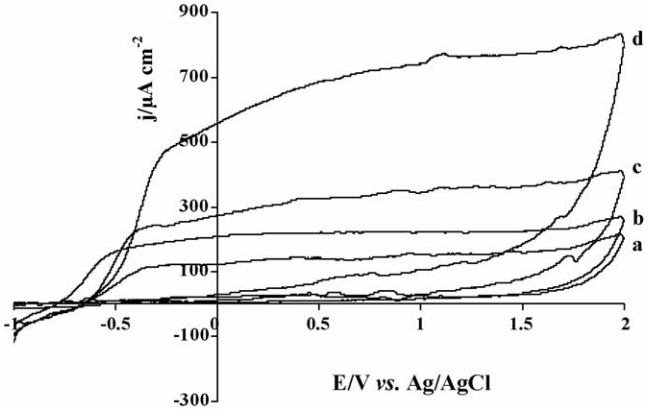

Fig. 3. Cyclic voltammograms (first scan) on Al electrode in 0.2 M $C_4H_6O_5$ medium at pH 2 with different scan rate: (a) 10 mV s^{-1}; (b) 20 mV s^{-1}; (c) 50 mV s^{-1}; (d) 100 mV s^{-1}.

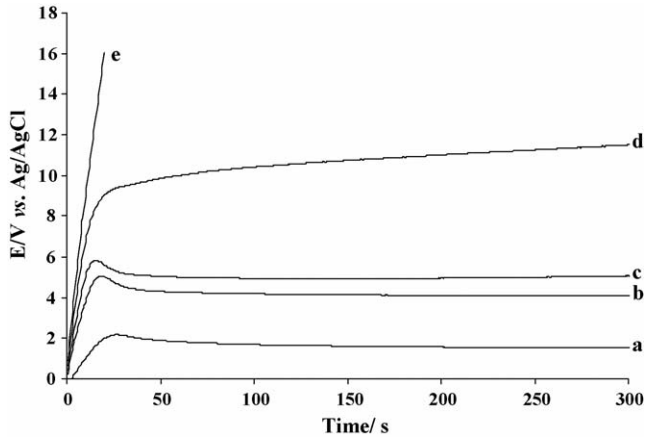

Fig. 4. Chronopotentiometric curves of pyrrole electropolymerization on Al in {0.2 M $C_4H_6O_5$ + 0.5 M Py} medium at pH 2 with different applied current densities: (a) 1 mA cm^{-2}; (b) 2 mA cm^{-2}; (c) 3 mA cm^{-2}; (d) 4 mA cm^{-2} and (e) 5 mA cm^{-2}.

change in the oxide layer of aluminium since the potential does not reach a plateau. It is important to stress that for 5 mA cm^{-2} of the applied current we couldn't obtain the Py electropolymerization because it has been attained the maximum potential of our equipment.

To ratify the mechanism of Al_2O_3/PPy formation, the transitions of the surface morphology was observed by SE and BE in the case of the applied current density of 3 mA cm^{-2}. In the initial stage (Q = 50 mC cm^{-2}), Fig. 5A, it is possible to observe PPy nuclei of 2 μm of diameter and few PPy islands of 8 μm of diameter. The X-ray analysis by EDS, Fig. 6A, confirms the presence of carbon in the dark zones of the micrograph obtained by backscattering electrons, which is associated to the organic polymer. In the sequent stage (Q = 125 mC cm^{-2}), Fig. 5B, the nuclei are now of 5 μm and PPy islands grow up to about 15 μm in diameter and begins to coalesce with one another, which is confirmed by EDS considering the increases of carbon peak in the dark zone, Fig. 6B. This suggests that conducting paths may exist under the PPy nuclei through Al_2O_3 layer [23]. After the passage of 250 mC cm^{-2} charge in the system, the nuclei are of 10 μm in diameter and about 35% of the electrode surface is covered with PPy, Fig. 5C. In the last stage (Q = 1.5 C cm^{-2}), Fig. 5D, the PPy coalesce to form a uniform film. Meanwhile, the film is not totally compact, since the EDS analysis of global surface, Fig. 6D, shows yet the presence of aluminium.

These results are in agreement with the already descript mechanism of the bilayer Al_2O_3/PPy. For larger time of electropolymerization the PPy islands agglutinate to develop a uniform and compact PPy film while the conducting path may become insulating.

Increasing the malic concentration decreases the time to attain the peak potential as also its value (Fig. 7). Indeed, the effects of complexation and to form a micelle promoting by the malate ions at the surface justify this behaviour. The effect of the PPy concentration on the galvanostatic process comes to ratify it (Fig. 8). It is remarked that with the 0.1 M Py concentration our system has been blocked, as a consequence of the attained potential due to the compactness and thickness of

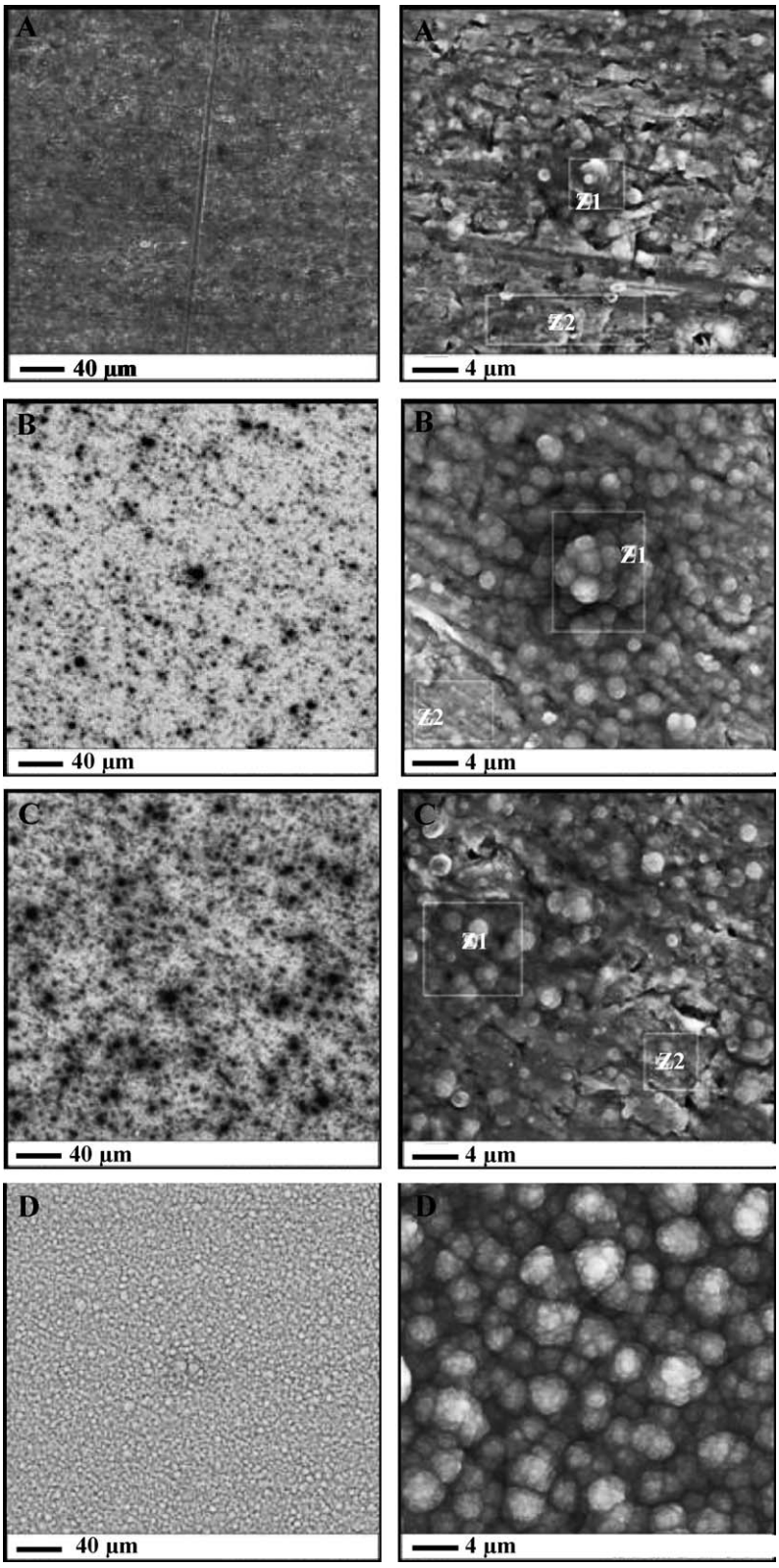

Fig. 5. SEM micrographs of the surface of aluminium electrode passed charge (Q) at (A) 50 mC cm^{-2}, (B) 125 mC cm^{-2}, (C) 250 mC cm^{-2}, and (D) 1.5 C cm^{-2}, in {0.2 M $C_4H_6O_5$ + 0.5 M Py} medium by applying a current density of 3 mA cm^{-2} at pH 2.

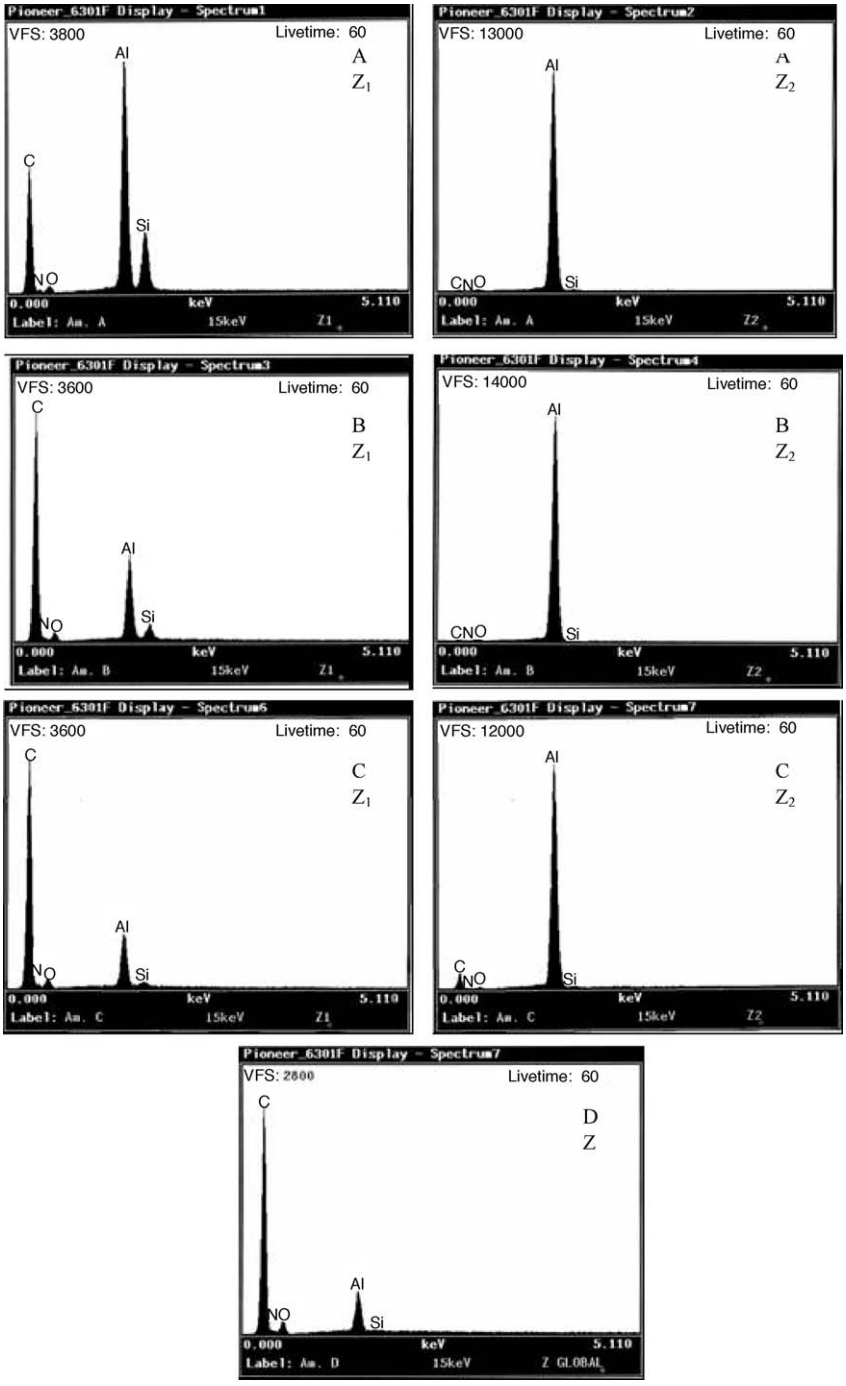

Fig. 6. EDS analysis of the surface of aluminium electrode passed charge (Q) at (A) 50 mC cm^{-2}, (B) 125 mC cm^{-2}, (C) 250 mC cm^{-2}, and (D) 1.5 C cm^{-2}, in $\{0.2\,\text{M}\ C_4H_6O_5 + 0.5\,\text{M Py}\}$ medium by applying a current density of 3 mA cm^{-2} at pH 2.

the barrier oxide, and consequently it was not achieved a PPy coating.

3.1.3. Potentiostatic deposition

In the case of potentiostatic mode only at potential higher than or equal to 2 V versus Ag/AgCl was obtained the Py electropolymerization in $\{0.2\,\text{M}\ C_4H_6O_5 + 0.5\,\text{M Py}\}$ medium at pH 2. The chronoamperometric curves (Fig. 9) show a decrease in current density, and then the nucleation and a growth of PPy on electrode surface take place. After this stage the current density increases, which is probably due to the growth of either independent nuclei or independent nuclei and simultaneous increases in number of nuclei. Since j increases approximately as t^2 it is possible to admit that the nucleation is progressive. Finally, the curves stretch out to a plateau, as a result of the competition of two opposing effects: growth of independent nuclei and overlap.

Figs. 10 and 11 show the influence of the Py and malic acid concentrations on the electropolymerization of pyrrole. It

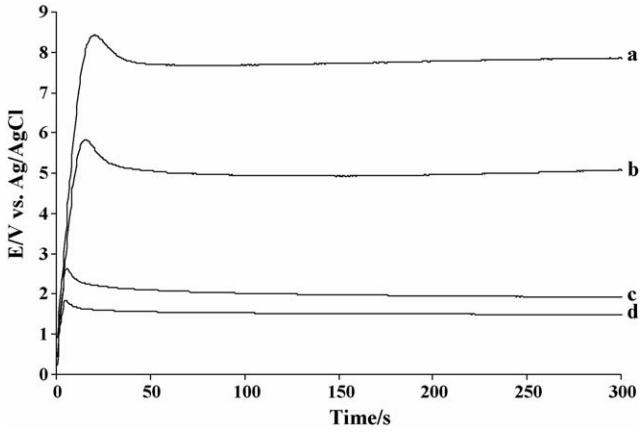

Fig. 7. Effect of the malic acid concentration in the galvanostatic electropolymerization of pyrrole on Al in 0.5 M Py medium at pH 2 by applying a current density of 3 mA cm^{-2}: (a) 0.1 M; (b) 0.2 M; (c) 0.4 M; (d) 0.8 M.

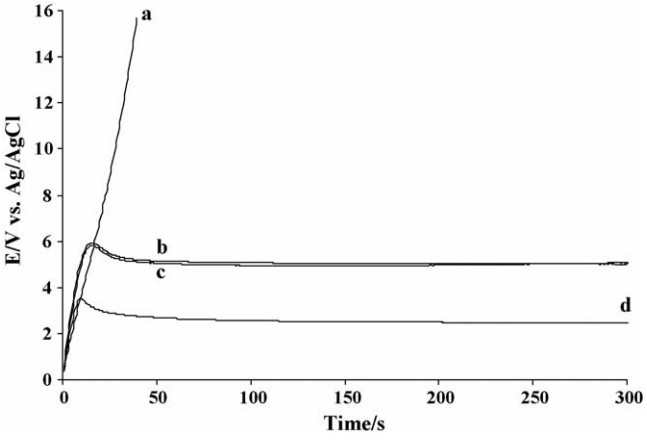

Fig. 8. Effect of the pyrrole concentration in the galvanostatic electropolymerization of pyrrole on Al in 0.2 M $C_4H_6O_5$ medium at pH 2 by applying a current density of 3 mA cm^{-2}: (a) 0.1 M; (b) 0.3 M; (c) 0.5 M; (d) 0.8 M.

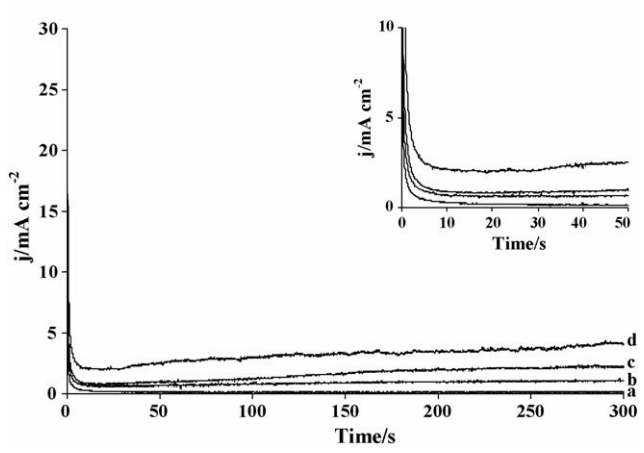

Fig. 9. Chronoamperometric curves of pyrrole electropolymerization on Al in {0.2 M $C_4H_6O_5$ + 0.5 M Py} medium at pH 2: (a) 0.7 V; (b) 1.4 V; (c) 2 V and (d) 4 V.

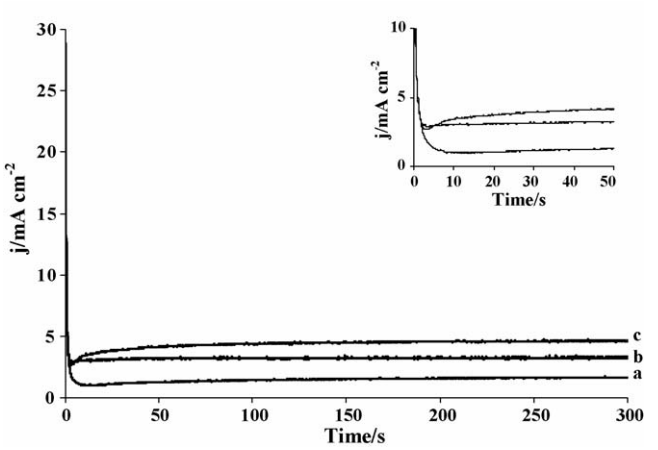

Fig. 10. Effect of the malic acid concentration in the potentiostatic electropolymerization of pyrrole in 0.5 M Py medium at pH 2 on Al by applying a potential of 4 V vs. Ag/AgCl: (a) 0.1 M; (b) 0.4 M; (c) 0.8 M.

is important to underline that it is necessary to have a Py concentration higher than 0.1 M to carry out the electrodeposition of PPy for all the applied electrochemical methods.

3.2. Corrosion performance

3.2.1. Linear polarization in 3% NaCl

The coated electrodes have been obtained galvanostatically at 4 mA cm^{-2} during 10 min in {0.2 M $C_4H_6O_5$ + 0.5 M pyrrole} medium and pH 2. The corrosion resistance of these coating samples and the aluminium was estimated by applying different current densities in 3% NaCl medium (Fig. 12) during 5 min. The obtained results give the possibility to deduce the following: (1) the bare Al electrode corrosion is higher than the PPy/Al-coated; (2) considering the potential at which the coating has been developed (Fig. 4), the PPy is partially overoxidized that increases the resistance of the bilayer (Al_2O_3/PPy) structure on aluminium and therefore a better behaviour against corrosion.

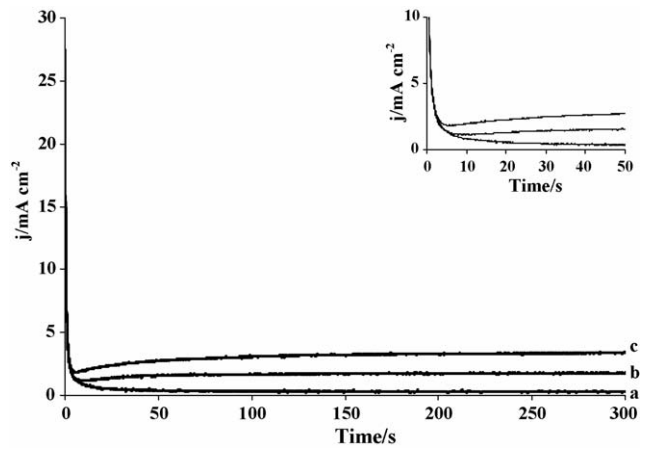

Fig. 11. Effect of the pyrrole concentration in the potentiostatic electropolymerization of pyrrole in 0.2 M $C_4H_6O_5$ medium at pH 2 on aluminium electrodes by applying a potential of 4 V vs. Ag/AgCl: (a) 0.1 M; (b) 0.3 M; (c) 0.8 M.

Table 2
Effect of conditions of pyrrole electropolymerization during 20 min on the capacity (C_s) and current leakage (L_c) determined at 120 Hz

Sample		C_s ($\mu F\,cm^{-2}$)	R ($k\Omega$)	L_c ($\mu A\,cm^{-2}$)
7	$j = 1\,mA\,cm^{-2}$; 0.2 M malic + 0.5 M Py	0.76	14	57
8	$j = 3\,mA\,cm^{-2}$; 0.2 M malic + 0.5 M Py	0.94	11	14
9	$j = 4\,mA\,cm^{-2}$; 0.2 M malic + 0.5 M Py	0.54	17	75
10	$j = 3\,mA\,cm^{-2}$; 0.1 M malic + 0.5 M Py	0.60	48	7.1
13	$j = 3\,mA\,cm^{-2}$; 0.8 M malic + 0.5 M Py	1.14	15	114
12	$V = 4$ V vs. Ag/AgCl; 0.4 M malic + 0.5 M Py	1.07	10	85
14	$V = 4$ V vs. Ag/AgCl; 0.8 M malic + 0.5 M Py	1.21	12	57

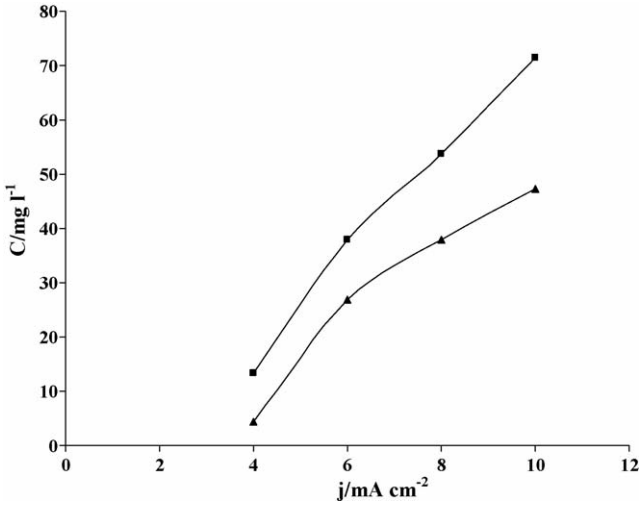

Fig. 12. Evolution of the Al concentration in solution with the applied current density in 3% NaCl during 5 min: (▲) Al bare, (■) PPy-coated Al.

3.3. Capacitive characteristics of PPy/Al_2O_3/Al

The Al_2O_3 barrier layer established on the aluminium anodizing is proportional to the potential, i.e., 14 Å V^{-1} [37]. In the case of the bilayer PPy/Al_2O_3 as discussed above, the cut-off potential (break down potential) define practically the thickness of the Al_2O_3 barrier layer [6]. Indeed, after the beginning of the Py electropolymerization the potential or current density stabilize at a plateau indicating a constant dielectric thickness.

It is known that the capacitance C can be connected with the barrier layer thickness e by the relation: $C = \varepsilon_r \varepsilon_o S/e$, where $\varepsilon_o = 8.85 \times 10^{-14}\,F\,cm^{-1}$ is the dielectric constant in vacuum, $\varepsilon_r = 10$ the relative constant for alumina and S (cm^2) is the electrode surface [38]. From the capacitive characteristics at 120 Hz of the produced capacitors, Table 2, in aqueous media of malic acid 0.2 M and Py 0.5 M, it is observed that the capacitance increases from 0.76 to 0.94 $\mu F\,cm^{-2}$ in the range of current density from 1 to 3 $mA\,cm^{-2}$ for the galvanostatic method. Considering the relation between C and e we believe that the compactness of the Al_2O_3 dielectric increases with the applied current density. This statement is in agreement with the decrease of the leakage current data and the increase of the capacitance values. The results obtained for the applied current density of 4 $mA\,cm^{-2}$ are in agreement with the observed evolution of the potential with the time, i.e., it was not obtained a plateau. It is evident that there is an alteration in the structure of the aluminium oxide. The influence of the malic acid concentration on the capacitive characteristics can be deduced from the analysis of the results of the capacitors 8, 10 and 13. It is obvious from the curves in Fig. 7 that the capacitance increases with the concentration conversely to the leakage current. This last behaviour is explained by the proposed mechanism for PPy growth on aluminium. Indeed, for conducting PPy coatings the established dendrites inside the Al_2O_3 structure are responsible for the larger leakage currents, which agree well with the observed potential in the curve d of Fig. 7.

In the case of the pontentiostatic method at 4 V versus Ag/AgCl, the capacitance increases with the concentration of the supporting electrolyte and the leakage current decreases.

4. Conclusions

Polypyrrole can be grown on aluminium surfaces in aqueous medium of Py concentration higher than 0.1 M using malic acid as supporting electrolyte under cyclic, galvanostatic or potentiostatic conditions. The mechanism concerned with pyrrole electropolymerization is consistent with a bilayer-film composed by a barrier-type Al_2O_3 and an electronically conducting PPy layer. It is possible, by changing the electropolimerization parameters and bath composition, to obtain adherent and homogeneous films that can be used as protective coatings against corrosion or as counter electrode in solid-state capacitors.

References

[1] H. Yamamoto, M. Oshima, T. Hosaka, I. Isa, Synth. Met. 104 (1999) 33.
[2] Y. Kudoh, T. Kojima, M. Fukuyama, S. Tsuyama, S. Tsuchiya, S. Yosshimura, J. Power Sources 60 (1996) 157.
[3] S. Niwa, Synth. Met. 18 (1987) 665.
[4] L.H.M. Krings, E.E. Havinga, J.J.T.M. Donkers, F.T.A. Vork, Synth. Met. 54 (1993) 453.
[5] M. Satoh, H. Ishikawa, K. Amano, E. Hasegawa, K. Yoshino, Synth. Met. 71 (1995) 2259.
[6] M.L. Tsai, P.J. Chen, J.S. Do, J. Power Sources 133 (2004) 302.
[7] H. Yamamoto, M. Oshima, M. Fukuda, I. Isa, K. Yoshino, J. Power Sources 60 (1996) 173.
[8] S. Niwa, Y. Taketani, J. Power Sources 60 (1996) 165.
[9] A. Dehbi, W. Wondrak, Y. Ousten, Y. Danto, Microel. Reliab. 42 (2002) 835.
[10] Y. Kudoh, M. Fukuyama, S. Yoshimura, Synth. Met. 66 (1994) 157.
[11] Y. Kudoh, S. Tsuciya, T. Kojima, M. Fukuyama, S. Yoshimura, Synth. Met. 41 (1991) 1133.
[12] M. Satoh, H. Ishikawa, H. Yageta, K. Amano, E. Hasegawa, Synth. Met. 84 (1997) 167.
[13] F. Larmat, J.R. Reynolds, Y.J. Qiu, Synth. Met. 79 (1996) 229.

[14] K.S. Jang, B. Moon, E.J. Oh, H. Lee, J. Power Sources 124 (2003) 338.
[15] M. Satoh, H. Ishikawa, H. Yageta, K. Amano, E. Hasegawa, K. Yoshino, Synth. Met. 65 (1994) 39.
[16] M. Satoh, H. Ishikawa, H. Yageta, K. Amano, E. Hasegawa, NEC Res. Dev. 36 (1995) 359.
[17] M. Bazzaoui, J.I. Martins, E.A. Bazzaoui, T.C. Reis, L. Martins, J. Appl. Electrochem. 34 (2004) 815.
[18] J.I. Martins, T.C. Reis, M. Bazzaoui, E.A. Bazzaoui, L. Martins, Corros. Sci. 46 (2004) 2361.
[19] M. Bazzaoui, E.A. Bazzaoui, J.I. Martins, L. Martins, Mat. Sci. Forum 455/456 (2004) 484.
[20] M. Bazzaoui, J.I. Martins, S.C. Costa, E.A. Bazzaoui, T.C. Reis, L. Martins, Electrochim. Acta 51 (2006) 2417.
[21] F. Beck, P. Hülser, J. Electroanal. Chem. 280 (1990) 159.
[22] K.M. Cheung, D. Bloor, G.C. Stevens, Polymer 29 (1988) 1709.
[23] K. Naio, M. Takeda, H. Kanno, M. Sakakura, A. Shimada, Electrochim. Acta 45 (2000) 3413.
[24] S.B. Saidman, J. Electroanal. Chem. 537 (2002) 39.
[25] S.B. Saidman, J.B. Bessone, J. Electroanal. Chem. 521 (2002) 87.
[26] G.S. Akundy, J.O. Iroh, Polymer 42 (2001) 9665.
[27] M. Bazzaoui, J.I. Martins, T.C. Reis, E.A. Bazzaoui, M.C. Nunes, L. Martins, Thin Solid Films 485 (2005) 155.
[28] P. Hülser, F. Beck, J. Appl. Electrochem. 20 (1990) 596.
[29] M.M. Lohrengel, Mater. Sci. Eng. R 11 (1993) 243.
[30] J.I. Martins, M. Bazzaoui, L. Martins, E.A. Bazzaoui, Européen Patent, 1227135, 2005.
[31] J.I. Martins, M. Bazzaoui, T.C. Reis, E.A. Bazzaoui, L. Martins, Synth. Met. 129 (2002) 221.
[32] M. Pourbaix, Atlas d'équilibres électrochimiques, Gauthier-Villars & Companie, Paris, 1963.
[33] E.M. Genies, G. Bidan, A.F. Diaz, J. Electroanal. Chem. 149 (1983) 101.
[34] F. Beck, Electrochim. Acta 33 (1988) 839.
[35] F. Beck, M. Oberst, R. Jansen, Electrochim. Acta 35 (1990) 1841.
[36] H.S. Fogler, Elements of Chemical Reaction Engineering, 3rd ed., Prentice-Hall, New Jersey, 1999.
[37] T. Endo, K. Kubo, S. Hiyama, FUJITSU Sci. Technol. J. 5 (1969) 87.
[38] J. Hitzig, K. Junttner, W.J. Lorentz, W. Paatsch, Corros. Sci. 24 (1984) 945.